Practical Model for Compressive Cake Filtration Including Fine Particle Invasion

Faruk Civan

School of Petroleum and Geological Engineering, The University of Oklahoma, T301 Energy Center, Norman, OK 73019

Practical and improved ordinary differential models for compressible filter cake buildup involving small particle invasion and deposition inside the cake at static and dynamic conditions are developed by averaging particle and carrier fluid transport equations over the filter cake thickness. The models are simplified by considering that the particles and carrier fluids involving many practical applications are incompressible. The results of radial and linear filtration cases are compared for constant rate and constant pressure drive filtrations. This thickness-averaged ordinary differential model reproduces the predictions of the Tien et al. (1997) partial differential model rapidly with less computational effort. Parametric studies indicate that the particle screening efficiency of the filter is an important factor on the filter cake properties and filtration rate, and differences between linear and radial cake filtration performances are more pronounced, and the cake thickness and filtrate volume are smaller for constant pressure filtration than constant rate filtration. The equations of the thickness-averaged linear and radial filter cake formation models are simple requiring less computational effort over the reported partial differential models for the analysis, design and optimization of the industrial cake filtration processes involving plate and drum filters.

Introduction

Frequently, the separation of particles from slurries is accomplished by filtration through a filter media that is impermeable for the particles but permeable for the carrier fluid. Filtration also occurs inherently in some processes. For example, hydraulic fracturing of petroleum-bearing rock and overbalanced drilling of wells into petroleum reservoirs usually cause a cross-flow filtration which leads to a filter cake buildup over the face of the porous rock and filtrate invasion into the reservoir (Civan, 1994, 1996). When the slurry contains particles of different sizes, the larger particles of the slurry form the skeleton of the filter cake and the smaller particles can migrate into and deposit within the porous cake formed by the large particles. Simultaneously, the cake may undergo a compaction process under the effect of the fluid drag as the suspension of smaller particles flows through the cake (Tien et al., 1997). Consequently, the porosity, permeability, and thickness of the cake vary, which in turn affect the performance of the filtration process. Static filtration occurs when a slurry is applied to a filter without cross-flow. Therefore, the particles are continuously deposited to form thicker filter cakes. Dynamic filtration involves some cross-flow. Therefore, the filter cake thickness varies until the particle deposition and erosion rates equal.

Many industrial filtration processes and instruments facilitate drum- and plate-type filters, made of porous materials, which involve radial and linear flow cases, respectively, although many other filtration techniques are also available (Chen, 1997). Model assisted analyses and interpretation of experimental data, and optimization and simulation of the filtration processes, are of continuing interest for the industry. The majority of the previous modeling efforts has been limited to linear filtration applications, in spite of the fact that many industrial filtration processes facilitate radial filtration applications. Linear filtration models can closely approximate radial filtration only when the thicknesses of the filter and filter cake are sufficiently small relative to the radius of the filter surface exposed to slurry. Otherwise radial models should be used for radial filtration.

Because of their simplicity, empirical correlations such as those reviewed by Clark and Barbat (1989) are frequently used for static and dynamic filtration. Xie and Charles (1997) have demonstrated that the use of a set of properly selected dimensionless groups leads to improved empirical correlations. However, such simplified models omit the internal details of the filtration processes, and, therefore, may lead to incorrect results if applied for conditions beyond the range of the experimental data used to obtain the empirical correlations. In many industrial applications, the phenomenological models describing the mechanisms of the cake formation based on the conservation laws and rate equations are preferred for filter cake buildup involving small particle migration and deposition and cake compaction, because these models allow for extrapolation beyond the range of data used to test and calibrate the models. Chase and Willis (1992), Sherman and Sherwood (1993), and Smiles and Kirby (1993) presented partial differential models for compressible filter cakes without particle intrusion. Liu and Civan (1996) developed a partial differential model for incompressible filter cake buildup, and filtrate and fine particle invasion into petroleum-bearing rock at dynamic condition. Tien et al. (1997) have developed a partial differential model for compressible filter cakes considering small particle retention inside the cake at static condition. The solutions of such partial differential models require complicated, time-consuming, and computationally intensive numerical schemes. To alleviate this difficulty, Corapcioglu and Abboud (1990), Abboud (1993), and Civan (1994) have resorted to formulations facilitating cake thickness averaging. Consequently, the partial differential filtration models have been reduced to ordinary differential equations requiring much less computational effort. Such mathematically simplified models are particularly advantageous, because ordinary differential equations can be solved rapidly, accurately, and conveniently by readily available and well established numerical methods. The thickness-averaged models developed by Corapcioglu and Abboud (1990) and Abboud (1993) consider a constant porosity and linear cake filtration at a static condition. The constant porosity assumption was justified by their filtration experiments, because they used very dilute suspensions of particles and low-pressure filtration near the atmospheric pressure. Their models would not be applicable for high-pressure filtration of thick slurries considered by Tien et al. (1997) and commonly practiced in many industrial filtration processes. Further, they assumed the same values for the rates of deposition of the small and large particles over the progressing filter cake surface. This assumption is invalid for most applications.

In the following, improved ordinary differential models incorporating the effects of filter cake compaction and small particle invasion and retention at static and dynamic conditions are developed by filter cake thickness averaging by extending the methodology by Corapcioglu and Abboud (1990) and Civan (1994, 1996). The new models alleviate the aforementioned problems associated with the previous models. Simplified forms of this model, considering that the particles and carrier fluid can be assumed incompressible for many practical applications, are also derived. The applications to radial and linear filtration processes are presented and the results are compared. It is demonstrated that the present thickness-averaged ordinary differential filter cake model can reproduce the predictions of the Tien et al. (1997) partial differential model rapidly with less computational effort.

Radial Filtration Formulation

Consider that a slurry is applied to the inner surface of a drum filter and the filtrate leaves from its outer surface. However, the model developed here is equally applicable for the reverse operation. The filter cake is located between the filter inner surface radius r_w (cm) over which the cake is formed, and the slurry side cake surface radius r_c (cm) and its thickness is denoted by $h = r_w - r_c$. The external surface radius of the filter from which the filtrate leaves is r_e (cm), and the filter width is indicated by w (cm) such that the area of the inner filter surface over which the cake is formed is $2\pi r_w w$. The slurry flows over the cake surface at a tangential or cross-flow velocity of v_f (cm/s) and the filtrate flows into the filter at a filtration velocity of u_f (cm^3/cm$^2\cdot$s) normal to the filter face due to the overbalance of the pressure between the slurry and the effluent sides of the filter. The flowing suspension of particles and the filter cake (solid) are denoted by the subscripts f and s, respectively. The carrier phase (liquid) and the particles are denoted, respectively, by l and p. Following Tien et al. (1997), the slurry is considered to contain particles larger than the filter medium pore size that form the filter cake and the particles smaller than the pore sizes of the filter cake, as well as the filter medium which can migrate into the cake and the filter to deposit there. All particles (small plus large) are denoted by p, and the large and small particles are designated by $p1$ and $p2$, respectively.

The radial mass balances of all particles forming the cake, the small particles retained within the cake, the carrier fluid, and the small particles suspended in the carrier fluid are given, respectively, by

$$\frac{\partial}{\partial t}(\epsilon_s \rho_p) + \frac{1}{r}\frac{\partial}{\partial r}(r\rho_p u_s) = R_{p2s} \tag{1}$$

$$\frac{\partial}{\partial t}(\epsilon_s c_{p2s}) + \frac{1}{r}\frac{\partial}{\partial r}(r c_{p2s} u_s) = R_{p2s} \tag{2}$$

$$\frac{\partial}{\partial t}(\epsilon_l \rho_l) + \frac{1}{r}\frac{\partial}{\partial r}(r\rho_l u_l) = 0 \tag{3}$$

$$\frac{\partial}{\partial t}(\epsilon_l c_{p2l}) + \frac{1}{r}\frac{\partial}{\partial r}(r c_{p2l} u_l) = -R_{p2s} \tag{4}$$

Equations 1 to 4 apply over the cake, located within $r_c \le r \le r_w$, and for $t > 0$. ϵ_s and ϵ_l denote the volume fractions of the bulk cake system occupied by the cake forming particles and the carrier fluid, respectively. ρ_p and ρ_l are the densities of the particles and the carrier fluid (g/cm^3). u_s and u_l are the volumetric fluxes of the compressing filter cake (cm/s) and the carrier fluid flowing through the cake (cm^3/cm$^2\cdot$s). c_{p2s} and c_{p2l} denote the small particle masses contained per unit volumes of the cake forming particles and the carrier fluid flowing through the cake (g/cm^3). R_{p2s} is the mass rate of small particle deposition per unit bulk volume of the cake system (g/s/cm^3). t and r denote the time (s) and radial distance (cm), respectively.

As the filter cake is formed, the slurry side cake surface moves backward against the slurry filtration direction. Thus, the boundary conditions for Eqs. 1 to 4, which apply at the progressing cake surface for $r = r_c(t)$ and $t > 0$ are given, respectively, by the following jump mass balance equations

$$0=(\rho_p)_c[(u_s)_c-(u_s^\sigma)_c]-R_{ps}^\sigma \tag{5}$$

$$0=(c_{p2s})_c[(u_s)_c-(u_s^\sigma)_c]-R_{p2s}^\sigma \tag{6}$$

$$(\rho_l)_{\text{slurry}}[(u_l)_{\text{slurry}}-(u_l^\sigma)_{\text{slurry}}]=(\rho_l)_c[(u_l)_c-(u_l^\sigma)_c] \tag{7}$$

$$(c_{p2l})_{\text{slurry}}[(u_l)_{\text{slurry}}-(u_l^\sigma)_{\text{slurry}}]=(c_{p2l})_c[(u_l)_c-(u_l^\sigma)_c]+R_{p2s}^\sigma \tag{8}$$

In Eqs. 5 to 8, the subscripts slurry and c denote the slurry and the cake sides of the filter cake surface exposed to the slurry being injected into the filter. The moving cake surface is denoted by the superscript σ.

The macroscopic (superficial) velocities of the filter cake surface, and the carrier fluid at the slurry and the cake sides, are given, respectively, by

$$(u_s^\sigma)_c=(\epsilon_s)_c dr_c/dt \tag{9}$$

$$(u_l^\sigma)_{\text{slurry}}=(\epsilon_l)_{\text{slurry}} dr_c/dt \tag{10}$$

$$(u_l^\sigma)_c=(\epsilon_l)_c dr_c/dt \tag{11}$$

R_{ps}^σ is the mass rate of particle deposition from the slurry over to the moving cake surface given by

$$R_{ps}^\sigma=R_{p1s}^\sigma+R_{p2s}^\sigma \tag{12}$$

where R_{p1s}^σ and R_{p2s}^σ denote, respectively, the mass rates of large and small particles deposition from the slurry over the cake surface (g/s/cm^2). R_{p2s}^σ is usually negligible unless the small particles are retained by a process of jamming of small particles across the pores of the large particles, such as described by Civan (1994, 1996) and Liu and Civan (1996).

The cake surface at contact with the filter is fixed. Hence

$$(u_s^\sigma)_w=(u_l^\sigma)_w=(u_l^\sigma)_{\text{filter}}=0 \tag{13}$$

Therefore, the filter side boundary conditions for Eqs. 1 to 4, which apply at $r=r_w$ and for $t>0$, are given, respectively, by

$$(u_s)_w=0 \tag{14}$$

$$(c_{p2s}u_s)_w=0 \tag{15}$$

$$(\rho_l u_l)_w=(\rho_l u_l)_{\text{filter}} \tag{16}$$

$$(c_{p2l}u_l)_w=(c_{p2l}u_l)_{\text{filter}} \tag{17}$$

Application of the thickness averaging rules given in Appendix A similar to Civan (1994) and the conditions given by Eqs. 5–17 yields the following cake thickness-averaged forms of Eqs. 1 to 4, respectively

$$\frac{d}{dt}\left[(r_w^2-r_c^2)\overline{\epsilon_s\rho_p}\right]=2r_cR_{ps}^\sigma+(r_w^2-r_c^2)\overline{R}_{p2s} \tag{18}$$

$$\frac{d}{dt}\left[(r_w^2-r_c^2)\overline{\epsilon_s c_{p2s}}\right]=2r_cR_{p2s}^\sigma+(r_w^2-r_c^2)\overline{R}_{p2s} \tag{19}$$

$$\frac{d}{dt}[(r_w^2-r_c^2)\overline{\epsilon_l\rho_l}]+(\rho_l\epsilon_l)_{\text{slurry}}\frac{dr_c^2}{dt}=2r_c(\rho_lu_l)_{\text{slurry}}-2r_w(\rho_lu_l)_{\text{filter}} \tag{20}$$

$$\frac{d}{dt}\left[(r_w^2-r_c^2)\overline{\epsilon_lc_{p2l}}\right]+(\epsilon_lc_{p2l})_{\text{slurry}}\frac{dr_c^2}{dt}=2r_c(c_{p2l}u_l)_{\text{slurry}}-2r_w(c_{p2l}u_l)_{\text{filter}}-2r_cR_{p2s}^\sigma-(r_w^2-r_c^2)\overline{R}_{p2s} \tag{21}$$

For many practical applications, it is reasonable to assume that the particles and the carrier fluid are incompressible. The volumetric retention rates of the large and small particles are given, respectively, by

$$N_{is}^\sigma=R_{is}^\sigma/\rho_p:\quad i=p,\,p1,\,p2 \tag{22}$$

$$N_{p2s}=R_{p2s}/\rho_p \tag{23}$$

The volumetric concentration (or fraction) of species i in phase j, the volume fraction of species i of phase j in the bulk of the cake system, and the superficial velocity of species i of phase j are given, respectively, by

$$\sigma_{ij}=c_{ij}/\rho_i \tag{24}$$

$$\epsilon_{ij}=\epsilon_j\sigma_{ij} \tag{25}$$

$$u_{ij}=u_j\sigma_{ij} \tag{26}$$

Substituting Eqs. 22 to 26 into Eqs. 18 to 21 leads to the following volumetric balance equations, respectively

$$\frac{d}{dt}[(r_w^2-r_c^2)\bar{\epsilon}_s]=2r_cN_{ps}^\sigma+(r_w^2-r_c^2)\overline{N}_{p2s} \tag{27}$$

$$\frac{d}{dt}\left[(r_w^2-r_c^2)\bar{\epsilon}_{p2s}\right]=2r_cN_{p2s}^\sigma+(r_w^2-r_c^2)\overline{N}_{p2s} \tag{28}$$

$$\frac{d}{dt}[(r_w^2-r_c^2)\bar{\epsilon}_l]+(\epsilon_l)_{\text{slurry}}\frac{dr_c^2}{dt}=2r_c(u_l)_{\text{slurry}}-2r_w(u_l)_{\text{filter}} \tag{29}$$

$$\frac{d}{dt}\left[(r_w^2-r_c^2)\bar{\epsilon}_{p2l}\right]+(\epsilon_{p2l})_{\text{slurry}}\frac{dr_c^2}{dt}=2r_c(u_{p2l})_{\text{slurry}}-2r_w(u_{p2l})_{\text{filter}}-2r_cN_{p2s}^\sigma-(r_w^2-r_c^2)\overline{N}_{p2s} \tag{30}$$

The variation of the filter cake thickness (cm) $h=r_w-r_c$ can be calculated using the variable radius, $r_c=r_c(t)$ of the slurry side filter cake surface.

Linear Filtration Formulation

The radial filter cake equations derived above can be readily converted to linear filter cake equations by means of the transformation given by

$$x=r^2,\quad h=x_w-x_c=r_w^2-r_c^2 \tag{31}$$

Thus, application of Eq. 31 to Eqs. 18–21 yields, respectively, the following thickness-averaged mass balance equations for the linear cake formation

$$\frac{d}{dt}\left(h\overline{\epsilon_s \rho_p}\right) = R^{\sigma}_{ps} + h\overline{R}_{p2s} \tag{32}$$

$$\frac{d}{dt}\left(h\overline{\epsilon_s c_{p2s}}\right) = R^{\sigma}_{p2s} + h\overline{R}_{p2s} \tag{33}$$

$$\frac{d}{dt}(h\overline{\epsilon_l \rho_l}) - (\epsilon_l \rho_l)_{\text{slurry}}\frac{dh}{dt} = (\rho_l u_l)_{\text{slurry}} - (\rho_l u_l)_{\text{filter}} \tag{34}$$

$$\frac{d}{dt}\left(h\overline{\epsilon_l c_{p2l}}\right) - (\epsilon_l c_{p2l})_{\text{slurry}}\frac{dh}{dt} = (c_{p2l}u_l)_{\text{slurry}} - (c_{p2l}u_l)_{\text{filter}} - R^{\sigma}_{p2s} - h\overline{R}_{p2s} \tag{35}$$

Similarly, Eqs. 27–30, respectively, become

$$\frac{d}{dt}(h\overline{\epsilon}_s) = N^{\sigma}_{ps} + h\overline{N}_{p2s} \tag{36}$$

$$\frac{d}{dt}(h\overline{\epsilon}_{p2s}) = N^{\sigma}_{p2s} + h\overline{N}_{p2s} \tag{37}$$

$$\frac{d}{dt}(h\overline{\epsilon}_l) - (\epsilon_l)_{\text{slurry}}\frac{dh}{dt} = (u_l)_{\text{slurry}} - (u_l)_{\text{filter}} \tag{38}$$

$$\frac{d}{dt}(h\overline{\epsilon}_{p2l}) - (\epsilon_{p2l})_{\text{slurry}}\frac{dh}{dt} = (u_{p2l})_{\text{slurry}} - (u_{p2l})_{\text{filter}} - N^{\sigma}_{p2s} - h\overline{N}_{p2s} \tag{39}$$

Volume fractions of the filter cake solids and pore fluid can be expressed in terms of the cake porosity, respectively, as

$$\overline{\epsilon}_s = 1 - \overline{\phi} \tag{40}$$

$$\overline{\epsilon}_f = \epsilon_l + \epsilon_{p2l} = \overline{\phi} \tag{41}$$

where $\overline{\phi}$ is the average cake porosity (cm^3/cm^3). The following expressions for the small particle volume flux and mass per carrier fluid volume can be written according to Eqs. 24–26, respectively, as

$$u_{p2l} = u_l \epsilon_{p2l}/\epsilon_l = u_l c_{p2l}/\rho_p \tag{42}$$

$$c_{p2l} = \rho_p \epsilon_{p2l}/\epsilon_l \tag{43}$$

Note that Eqs. 18, 28 and 24 of Corapcioglu and Abboud (1990) correspond to the present Eqs. 32, 38 and 35, respectively, with some differences. Equation 32 simplifies to their Eq. 18, assuming ρ_p is constant and substituting Eq. 40. The present Eqs. 35 and 38 simplify to their Eqs. 24 and 28, substituting Eq. 41 for $\epsilon_{p2l} \ll \epsilon_l$. Also, Corapcioglu and Abboud (1990) did not distinguish between the rates of deposition of small and all (large plus small) particles over the progressing cake surface, that is, R^{σ}_{p2s} and R^{σ}_{ps}, and used $R^{\sigma}_{p2s} = R^{\sigma}_{ps}$ in their Eq. 24. This assumption is not valid, because most small particles migrate into the cake and only a little fraction of the small particles can deposit by the jamming process over the slurry side of the filter cake, such as described by Civan (1996). The filter cake is essentially formed by the deposition of the large particles, and the deposition of the small particles over the progressing cake surface is negligible. The deposition of the small particles more dominantly occurs within the cake matrix as the suspension of small particles flows through the cake. Therefore, there is a big order of magnitude difference between the rates of the small and large particles deposition over the filter cake, that is, $R^{\sigma}_{p1s} \gg R^{\sigma}_{p2s}$ and, thus, $R^{\sigma}_{ps} \cong R^{\sigma}_{p1s}$. However, it is more accurate to use

$$R^{\sigma}_{ps} = R^{\sigma}_{p1s} + R^{\sigma}_{p2s} \tag{44}$$

Pressure-Flow Relationships

The slurry carrier fluid flow rate u_l (cm^3/cm^2·s) can be expressed using the effluent fluid pressure p_e (atm) at the outlet side of the filter, the pressure p_c (atm) at the slurry side cake surface, and the harmonic average permeability of the cake and filter system in Darcy's law. Hence, the following expressions are obtained for the radial and linear cases, respectively

$$(u_l)_{\text{slurry}} = \frac{(\epsilon_l)_{\text{slurry}}\overline{k}_c(p_c - p_e)}{r_c \mu\left[\ln\left(\frac{r_w}{r_c}\right) + \frac{\overline{k}_c}{k_f}\ln\left(\frac{r_e}{r_w}\right)\right]} \tag{45}$$

$$(u_l)_{\text{slurry}} = \frac{(\epsilon_l)_{\text{slurry}}\overline{k}_c(p_c - p_e)}{\mu\left(h + \frac{\overline{k}_c}{k_f}L_f\right)} \tag{46}$$

where μ is the viscosity (cp) of the suspension of small particles flowing through the cake which is approximated as the viscosity of the carrier fluid for dilute suspensions, k_f is the filter permeability (darcy), h is the cake thickness, and L_f is the filter thickness (cm).

Similarly, the following relationships can be written for the carrier fluid flow through the filter media, in the radial and linear cases, respectively

$$(u_l)_{\text{filter}} = \frac{(\epsilon_l)_{\text{filter}}k_f(p_w - p_e)}{\mu r_w \ln\left(\frac{r_e}{r_w}\right)} \tag{47}$$

$$(u_l)_{\text{filter}} = \frac{(\epsilon_l)_{\text{filter}}k_f(p_w - p_e)}{\mu L_f} \tag{48}$$

where p_w denotes the pressure at the cake side filter surface (atm).

Finally, for thin cakes, the average fluid pressure inside the cake can be estimated by an arithmetic average as

$$\overline{p} = (p_w + p_c)/2 \tag{49}$$

For thick cakes, the average fluid pressure can be calculated by the formula derived in Appendix B. Then, the average drag force exerted on the cake particles can be estimated according to Tiller and Crump (1985) by

$$\bar{p}_s = p_c - \bar{p} \tag{50}$$

Equation 50 is later utilized in Eqs. 58 and 59 to account for the effects of the cake compaction on the porosity and permeability of the filter cake.

Particle Deposition Rates

The rate of deposition of the particles of the slurry over the slurry side cake surface is assumed proportional to the particle mass flux approaching the filter cake. The rate of erosion of the particles from the slurry side cake surface is assumed proportional to the tangential, excess shear stress above the critical stress necessary for particle mobilization. Therefore, for dynamic filtration involving cross-flow, the net mass rate of all particles (large plus small) deposition per unit area of the slurry side cake surface is given by the difference between the deposition and erosion rates as (Civan, 1996)

$$R_{ps}^{\sigma} = k_d^{\sigma}(u_l c_{pl})_{\text{slurry}} - k_e^{\sigma}(\epsilon_s p_p)_c (\tau - \tau_{cr}) U(\tau - \tau_{cr}) \tag{51}$$

where k_d^{σ} and k_e^{σ} denote the deposition (dimensionless) and erosion rate ($g^{-1} \cdot cm^2 \cdot s$) coefficients, u_l is the carrier fluid filtration flux normal to the cake surface ($cm^3/cm^2 \cdot s$), c_{pl} is the slurry particle concentration expressed as the particle mass per unit volume of the carrier fluid in the slurry, τ_{cr} is the minimum shear stress required for particle mobilization ($dyne/cm^2$), τ is the shear-stress applied by the slurry cross-flow over the filter cake ($dyne/cm^2$), and U is a unit step function. The non-Newtonian fluid shear stresses for radial and linear filter cakes are given by the Rabinowitsch-Mooney equation (Metzner and Reed, 1955), respectively, as

$$\tau = k'(4v/r_c)^{n'} \tag{52}$$

$$\tau = k'(8v)^{n'} \tag{53}$$

where k' and n' are the consistency ($dyne/cm^2/s^{n'}$) and flow (dimensionless) indices, which are equal to the fluid viscosity μ and unit for Newtonian fluids, respectively, v is the tangential velocity of the slurry over the filter cake surface. For static filtration, $v = 0$ and therefore $\tau = 0$, and the second term on the right side of Eq. 51 drops out, leading to an expression similar to Corapcioglu and Abboud (1990) and Tien et al. (1997).

For small particles retention over the slurry side of the cake, an expression similar to Eq. 51 can be written as

$$R_{p2s}^{\sigma} = k_{d2}^{\sigma}(u_l c_{p2l})_{\text{slurry}} - k_{e2}^{\sigma}(\epsilon_s c_{p2s})_c (\tau - \tau_{cr2}) U(\tau - \tau_{cr2}) \tag{54}$$

in which $(c_{p2l})_{\text{slurry}}$ denotes the mass of small particles per volume of the carrier fluid in the slurry. The other parameters are defined similarly to those shown in Eq. 51.

The net mass rate of deposition of small particles within the filter cake is given by

$$\bar{R}_{p2s} = \bar{k}_d \bar{\epsilon}_l \bar{c}_{p2l} - \bar{k}_e \bar{\epsilon}_s \bar{c}_{p2s} \tag{55}$$

which is similar to Eq. 33 of Corapcioglu and Abboud (1990), but the deposition and the mobilization terms are more consistently expressed.

Following Ravi et al. (1992), the critical shear stress necessary for detachment of the deposited particles from the progressing cake surface can be estimated according to Potanin and Uriev (1991) by

$$\tau_{cr} = H/(24dl^2) \tag{56}$$

where $H = 3.0 \times 10^{-13}$ erg is the Hamaker coefficient, d is the average particle diameter (cm), and l is the separation distance (cm) between the particle surfaces. However, the actual critical stress can be several fold different than predicted by Eq. 56, because the ideal theory neglects the effects of the other factors, including aging (Ravi et al., 1992), surface roughness, and particle stickiness (Civan, 1996), on the particle detachment. Therefore, Ravi et al. (1992) recommend that the critical shear stress be determined experimentally.

Porosity and Permeability Relationships

Arshad (1991) generalized Adin's (1978) equation by considering the packing inefficiency resulting in the formation of the dead-end pores which do not conduct fluid. This equation can be applied for the variation of the cake porosity by deposition of small particles as

$$\frac{\bar{\phi}}{\phi^o} = 1 - \alpha \left(\frac{\epsilon_{p2s}}{\phi^o} \right)^n \tag{57}$$

where ϕ^o is the porosity (cm^3/cm^3) of the cake without small particle deposition and compaction, and α and n are some empirical parameters. The empirical correlation given by Adin (1978) indicates that $\alpha = 1$ and $n = 1/2$.

Tien et al. (1997) expressed the variation of the cake porosity by compaction by

$$\frac{\bar{\epsilon}_s}{\epsilon_s^o} = \frac{1 - \bar{\phi}}{1 - \phi^o} = \left(1 + \frac{\bar{p}_s}{p_a} \right)^{\beta} \tag{58}$$

where $\bar{p}_s$ (atm) is the average compressive stress applied to the cake particles by the fluid flowing through the cake, given by Eq. 50, and p_a (atm) and β are some empirical parameters.

Assuming that the stress and deposition effects are separable, Eqs. 57 and 58 can be combined as

$$\frac{\bar{\phi}}{\phi^o} = \left[1 - \alpha \left(\frac{\bar{\epsilon}_{p2s}}{\phi^o} \right)^n \right] \left[\frac{1}{\phi^o} - \left(\frac{1}{\phi^o} - 1 \right) \left(1 + \frac{\bar{p}_s}{p_a} \right)^{\beta} \right] \tag{59}$$

The permeability of the filter cake is estimated by means of the empirical relationship given by Tien et al. (1997)

$$\bar{k}_c / k_c^o = (1 + \alpha_1 \bar{\epsilon}_{p2s}^{\alpha_2})^{-1} (1 + \bar{p}_s/p_a)^{-\delta} \tag{60}$$

where α_1, α_2, β, and δ are some empirical parameters, and k^o is the cake permeability with no compaction and small particle deposition.

Applications

Corapcioglu and Abboud (1990) obtained a numerical solution for the linear constant rate filtration problem involving small particle invasion at a static condition, assuming that the cake is incompressible, the cake porosity remains constant, and all particles are filtered. Abboud (1993) repeated a similar calculation, but considered also the effect of small particles migration into the filter. Tien et al. (1997) considered both constant rate- and constant pressure-driven compressive cake filtrations in a linear and static case only.

In the following, the applications to constant rate- and constant pressure-driven filtration processes in linear and radial cases are presented and compared. The data considered in the present study are composed from the data used by Corapcioglu and Abboud (1990), Tien et al. (1997), and the missing data estimated in this study, as shown in Table 1. The best estimates of the missing data have been obtained by fitting the model to data as practiced by Liu and Civan (1996) and Tien et al. (1997). Development of better methods for unique determination of the model parameters for compressible cake filtration is an important issue, but beyond the scope of the present work. For example, Civan (1998) presents a methodology for determination of the model parameters for incompressive cake filtration by constructing various linear diagnostic charts from experimental data.

The numerical solutions of the ordinary differential Eqs. 36, 37, and 39 for the linear model and Eqs. 27, 28, and 30 for the radial model are obtained using the Runge-Kutta-Fehlberg four (five) method (Fehlberg, 1969) to determine

Table 1. Model Input Parameters

Parameter	Symbol	Data I	Data II
Cake porosity without compaction and small particle retention, cm^3 pore volume/cm^3 bulk volume	$\phi^o = 1 - \epsilon_s^o$	0.39**	0.73†
Cake particle volume fraction, cm^3 particle/cm^3 bulk volume	$\epsilon_s^o = 1 - \phi^o$	0.61†	0.27‡
Particle density, g/cm^3	ρ_p	1.18**	1.18*
Carrier fluid (water) density, g/cm^3	ρ_l	0.97**	0.97*
Slurry total particle mass fraction, g particles/g slurry	$(w_{pf})_{\text{slurry}}$	0.101**	—
Slurry total particle volume fraction, cm^3 particles/cm^3 slurry	$(\sigma_{pf})_{\text{slurry}}$	—	0.2‡
Slurry total particle mass per carrier fluid volume, g particle/cm^3 carrier fluid	$(c_{pl})_{\text{slurry}} = \frac{(w_{pf})_{\text{slurry}}\rho_l}{1-(w_{pf})_{\text{slurry}}} = \rho_p\left[\frac{1}{(\epsilon_l)_{\text{slurry}}} - 1\right]$	0.109†	0.295†
Slurry carrier fluid volume fraction, cm^3 carrier fluid/cm^3 slurry	$(\epsilon_l)_{\text{slurry}} = [1+(c_{pl})_{\text{slurry}}/\rho_p]^{-1} = (1-(\sigma_{pf})_{\text{slurry}}$	0.915†	0.8†
Slurry carrier fluid volumetric flux, cm^3 carrier fluid/(cm^2 cake surface·s)	$(u_l)_{\text{slurry}}$	2.0×10^{-3}**	2.0×10^{-3}‡
Slurry injection pressure, atm	p_c	8.9*	8.9‡
Filter outlet pressure, atm	p_e	1.0*	1.0‡
Slurry small particles mass per carrier fluid volume, g small particles/cm^3 carrier fluid	$(c_{p2l})_{\text{slurry}} = (\rho_p\sigma_{p2l})_{\text{slurry}}$	0.049*	0.059*
Slurry small particles volume per carrier fluid volume, cm^3 small particles/cm^3 carrier fluid	$(\sigma_{p2l})_{\text{slurry}} = (c_{p2l}/\rho_p)_{\text{slurry}}$	0.415†	0.05‡
Filtrate small particle mass per carrier fluid volume, g small particle/cm^3 carrier fluid	$(c_{p2l})_{\text{filter}}$	0, 0.005*	0, 0.005*
Filter thickness, cm	L_f	0.5*	0.5*
Slurry side filter radius, cm	r_w	5.08*	—
Filtrate side filter radius, cm	r_e	2.54*	—
Rate constant for small particle deposition within the cake, s^{-1}	$\bar{k}_d$	6.5×10^{-3}**	1.0×10^{-3}*,‖ 1.0×10^{-6}*,§
Rate constant for small particle entrainment within the cake, s^{-1}	$\bar{k}_e$	4.35×10^{-5}	5.0×10^{-5}*,‖ 5.0×10^{-7}*,§

*Data assumed.
**Corapcioglu and Abboud (1990).
†Data calculated.
‡Tien et al. (1997).
††Adin (1978).
§Data for the constant pressure case.
‖Data for the constant rate case.
#Static filtration.

Table 1. Model Input Parameters (Continued)

Parameter	Symbol	Data I	Data II
Rate constant for total particle deposition over the slurry side cake surface, dimensionless	k_d^σ	1.0*	1.4*,‖ 75.*,§
Rate constant for total particle erosion over the slurry side cake surface, $g^{-1}\cdot cm^2\cdot s$	k_e^σ	0#	0#
Rate constant for small particle deposition over the slurry side cake surface, dimensionless	k_{d2}^σ	0.1*	0.05*,‖ 0*,§
Rate constant for small particle erosion over the slurry side cake surface, $g^{-1}\cdot cm^2\cdot s$	k_{e2}^σ	0#	0#
Parameter in Eq. 60, dimensionless	α_1	30*	30.0‡
Parameter in Eq. 60, dimensionless	α_2	1*	1.0‡
Parameter in Eq. 58, dimensionless	β	0.09*	0.07*
Parameter in Eq. 60, dimensionless	δ	0.49*	0.47*
Cake permeability without compaction and small particle deposition, darcy	k_c^o	3.5×10^{-3}*	3.5×10^{-3}‡
Filter permeability, darcy	k_f	1.0×1.0^{-4}*	1.0×1.0^{-4}*
Viscosity of carrier fluid (water), cp	μ	1.0*	1.0*
Parameter in Eq. 57, dimensionless	α	1.0††	1.0††
Parameter in Eq. 57, dimensionless	n	1/2††	1/2††
An empirical constant in Eq. 58, atm	p_a	∞*	0.0118‡
A constant in Eqs. 52 and 53, $dyne/cm^2/s^{n'}$	k'	1.0*	1.0*
A constant in Eqs. 52 and 53, dimensionless	n'	1.0*	1.0*
Tangential velocity of the injected slurry, cm/s	ν	0, 0.01*	0, 0.01*

*Data assumed.
**Corapcioglu and Abboud (1990).
†Data calculated.
‡Tien et al. (1997).
††Adin (1978).
§Data for the constant pressure case.
‖Data for the constant rate case.
#Static filtration.

the filter cake thickness $h \equiv x_w - x_c$ for the linear and $h \equiv r_w - r_c$ for radial cases, and the volume fractions of the small particles retained in the cake and suspended in the flowing slurry $\bar{\epsilon}_{p2s}$ and $\bar{\epsilon}_{p2l}$, respectively. Equations 38 and 29 are used to determine the filtrate carrier fluid volumetric flux, $(u_l)_{\text{filter}}$ for the linear and radial cases, respectively. First, using the data given in Table 1, identified as Data I, the numerical solutions are carried out with the present, improved model, for both linear and radial constant rate filtrations. The results for all particles filtered, for which $(c_{p2l})_{\text{filter}} = 0$, as expected from an efficient filter, are compared and the effect of fine particle invasion into an inefficient filter is demonstrated by assuming a value of $(c_{p2l})_{\text{filter}} = 0.005$ g/cm^3 in Figures 1 to 5. The present results have similar trends, but different values than the results of Corapcioglu and Abboud (1990) and Abboud (1993), because of the simplifying assumptions involved in their calculations such as incompressible cake and constant cake porosity and the use of the same rates of deposition for small and all (large plus small) particles over the progressing cake surface. The present calculations are a step improvement, because their assumptions do not generally hold. Also, the average porosity of the filter cake can vary significantly in actual cases as described by Tien et al. (1997). Next, the numerical solution is obtained for the constant pressure drive filtration. Corapcioglu and Abboud (1990) and Abboud (1993) did not present any results for this case. The flow rate is allowed to vary according to Eqs. 45 and 46 for the radial and linear cases, respectively. In Figures 6 to 10, the results for the linear and radial cases are compared. The results presented in Figures 1 to 10 indicate that fine particle invasion into the filter plays an important role. The differences between the radial and linear filtration results are more pronounced and the cake thickness and filtrate volume are less for the constant pressure filtration.

Tien et al. (1997) have solved their partial differential model numerically using a ready-made Fortran subroutine for linear filtration at static condition and reported numerical solutions along the filter cake only at the 100 and 1,000 s times.

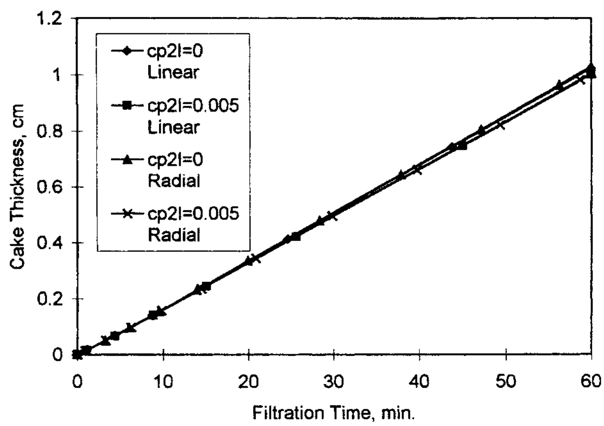

Figure 1. Cake thickness for linear and radial constant rate filtration.

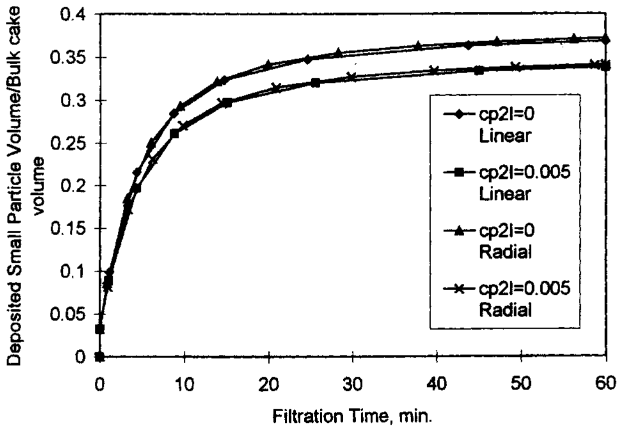

Figure 2. Small particle deposition for linear and radial constant rate filtration.

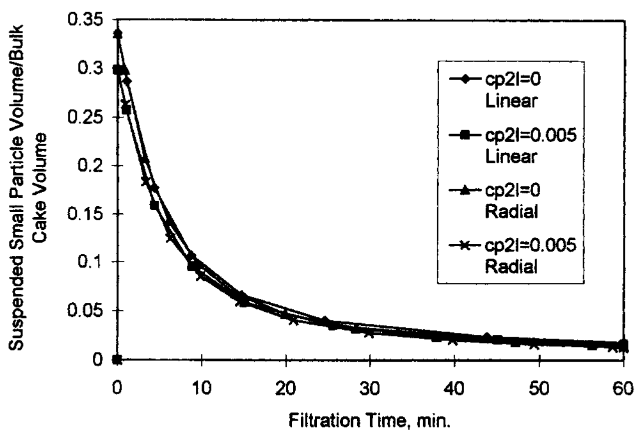

Figure 3. Suspended small particles for linear and radial constant rate filtration.

Their model generates numerical solutions over the thickness of the filter cake, whereas the present models calculate the thickness-averaged values. Therefore, the profiles predicted by Tien et al. (1997) have been averaged over the cake thickness and used for comparison with the solutions obtained with the present thickness-averaged filter cake model. Because they reported numerical solutions at only two time instances, this resulted with only two discrete values. The numerical so-

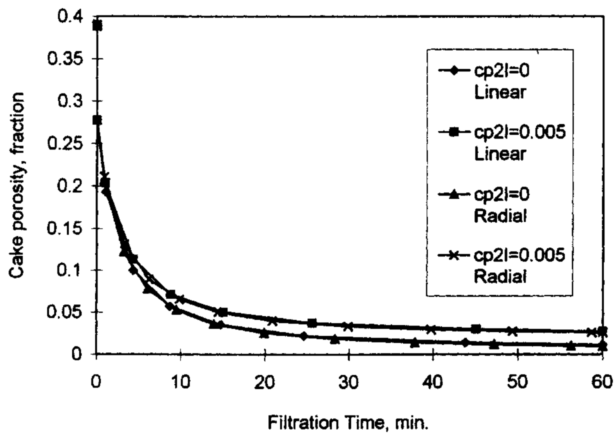

Figure 4. Cake porosity for linear and radial constant rate filtration.

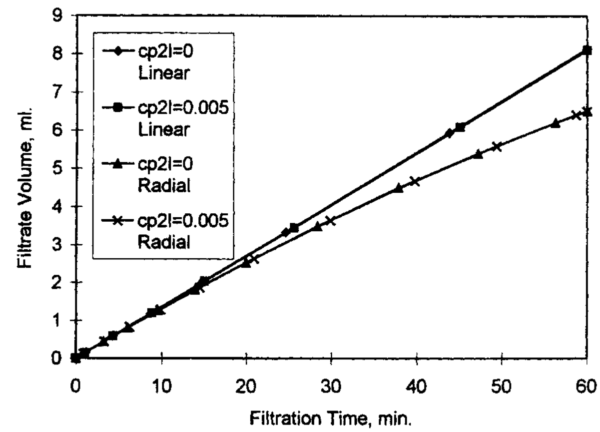

Figure 5. Filtrate volume for linear and radial constant rate filtration.

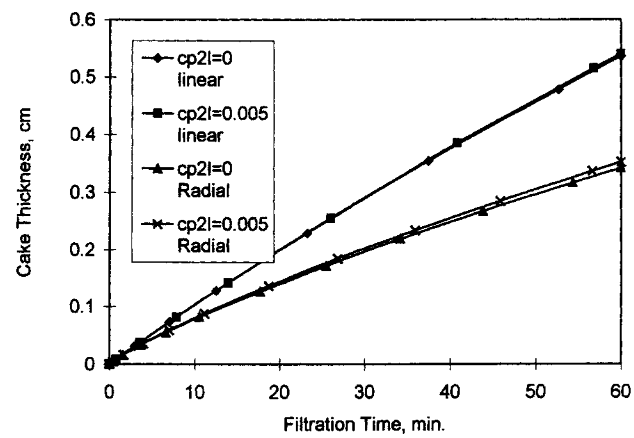

Figure 6. Cake thickness for linear and radial constant pressure filtration.

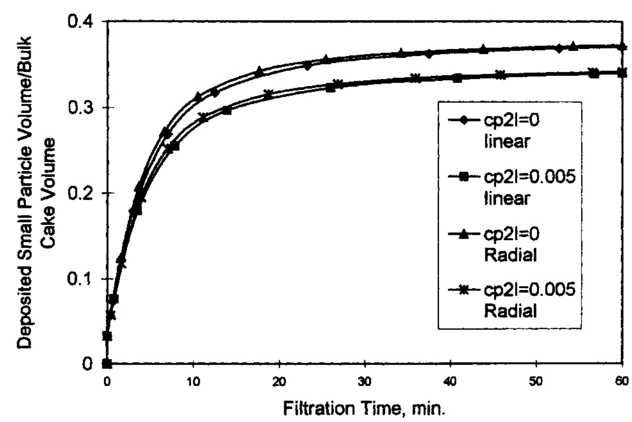

Figure 7. Small particle deposition for linear and radial constant pressure filtration.

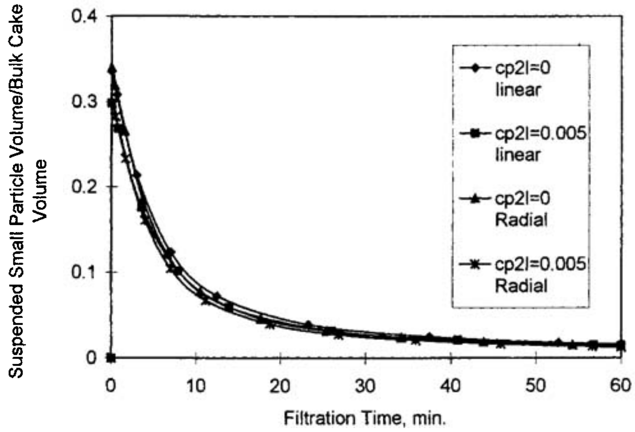

Figure 8. Suspended small particles for linear and radial constant pressure filtration.

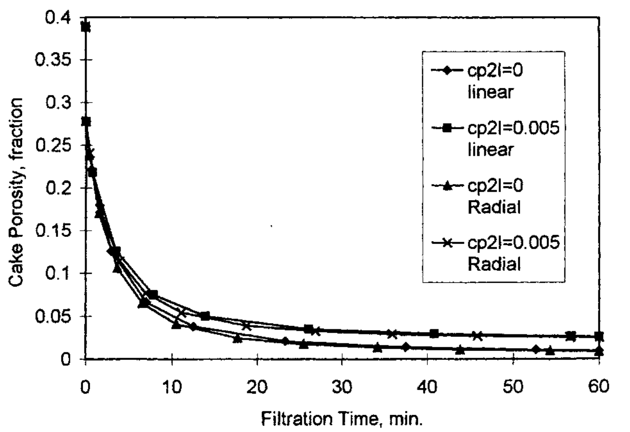

Figure 9. Cake porosity for linear and radial constant pressure filtration.

lutions were generated with the present linear filtration model using the data identified as Data II in Table 1 for constant rate and constant pressure filtrations. As can be seen by the results presented in Figures 11 to 14, the present ordinary differential model can closely reproduce the results of the Tien et al. (1997) partial differential model. Note that, as indicated in Table 1, the values of the parameters at the present cake thickness-averaged level should be different than those for the formulation at the local level considering the spatial variations, such as by Tien et al. (1997).

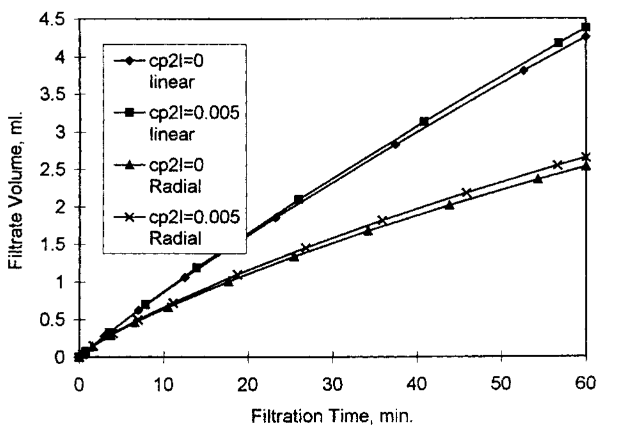

Figure 10. Filtrate volume for linear and radial constant pressure filtration.

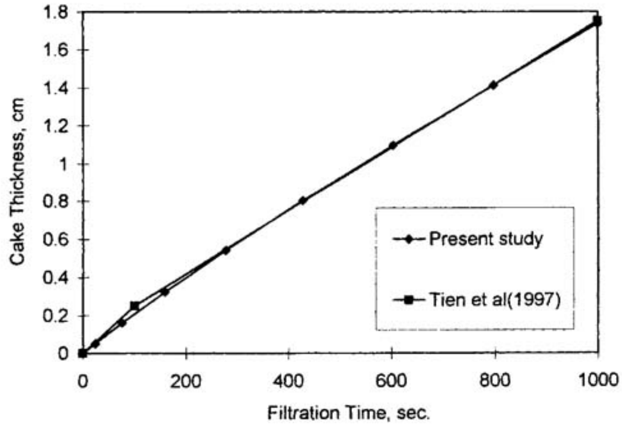

Figure 11. Cake thickness for constant rate filtration.

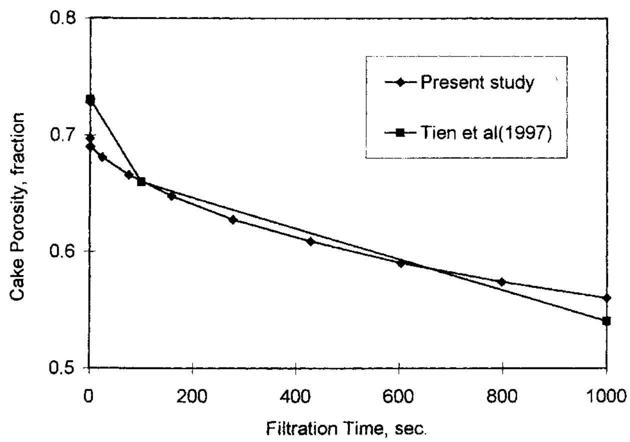

Figure 12. Cake porosity for constant rate filtration.

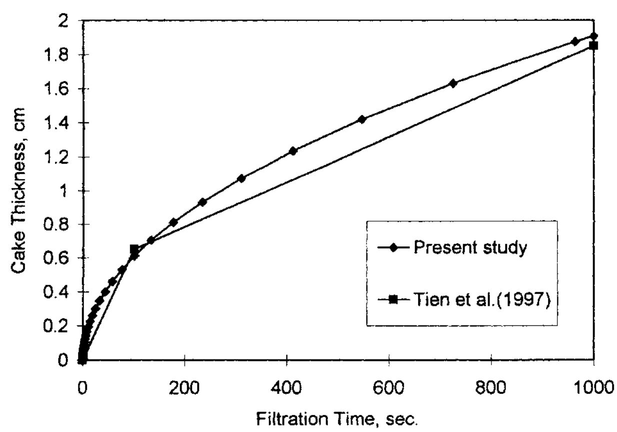

Figure 13. Cake thickness for constant pressure filtration.

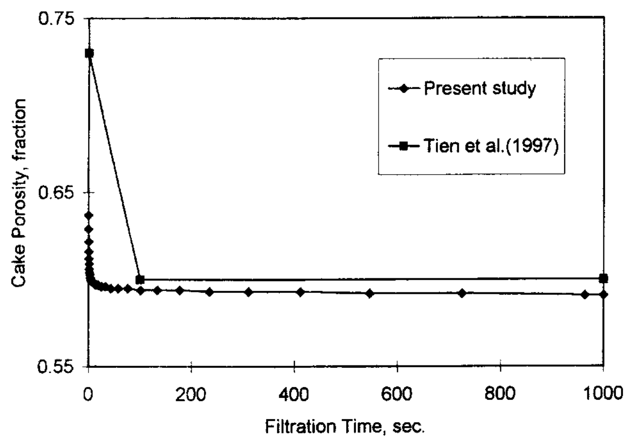

Figure 14. Cake porosity for constant pressure filtration.

Conclusions

Because of the improved phenomenological description and convenient cake thickness-averaged formulation, the present ordinary differential models can provide faster numerical solutions with reduced computational effort and, therefore, offer certain practical advantages over the previous models for the analysis, design, and optimization of the industrial cake filtration processes.

The applicability of the models by Corapcioglu and Abboud (1990) and Abboud (1993) is limited to static and low-pressure filtration of dilute suspensions and their assumption of the same rates for the deposition of the small and large particles over the progressing cake surface is not reasonable. The Tien et al. (1997) model can alleviate these problems, but it is computationally intensive and also limited to static filtration. These models are for linear filtration and may sufficiently approximate radial filtration only when the cake and the filter are much thinner compared to the radius of the filter surface exposed to the slurry. However, the radial model developed in this work can better describe the radial filtration involving thick filter cake and filter media.

It is concluded that the filtration models developed in this article provide insight into the mechanism of compressive cake filtration and a convenient means of simulation with additional features.

Acknowledgment

The author gratefully acknowledges the support of the School of Petroleum and Geological Engineering at the University of Oklahoma.

Notation

c_p = particle mass concentration in the slurry in total particle mass per carrier fluid volume, g/cm^3
c_{p2s} = small particle mass per volume of cake solid matrix, g/cm^3
c_{p2l} = small particle mass per volume of carrier fluid, g/cm^3
k' = consistency constant, dyne/cm^2/s$^{n'}$
k_c = filter cake permeability, darcy
k_e = erosion rate constant, s^{-1}
k_d^σ = rate constant for particle deposition over the cake surface, dimensionless
L_f = filter media length, cm
n' = flow index, dimensionless
N_{is}^σ = volumetric rate of deposition of particle species over the cake surface, cm^3/cm^2/s
N_{p2s} = volumetric rate of deposition of small particles inside the cake, cm^3/cm^3/s
N_{ps}^σ = volumetric rate of deposition of particles over the cake surface, cm^3/cm^2/s
N_{p2s}^σ = volumetric rate of deposition of small particles over the cake surface, cm^3/cm^2/s
p = pressure, atm
p_a = constant in Eq. 58, atm
p_w = pressure at the slurry side of the filter, atm
R_{ps}^σ = net mass rate of total particle addition at the filter cake surface, g/s/cm^2
u_s = macroscopic velocity of deforming solid phase, cm/s
u^σ = macroscopic velocity of the dividing surface, cm^3/cm$^2\cdot$s
u_{ij} = superficial velocity of species i of phase j
x = linear distance, cm
α_1, α_2 = dimensionless constants in Eq. 60
ϵ_l = volume fraction of the carrier fluid phase in the bulk media
ϵ_{ij} = volume fraction of species i of phase j in the bulk system
ϵ_s = fractional volume of the solid matrix in the bulk filter cake
ϵ_{p2l} = volume fraction of small particles of the carrier fluid
σ_{ij} = volume fraction of particle species i in phase j
ϕ_c = filter cake porosity, cm^3/cm^3
ρ_p = density of particle, g/cm^3
ρ_l = density of the carrier fluid, g/cm^3
μ = viscosity of fluid, cp
ν_f = slurry cross-flow or tangential velocity, cm/s

Subscripts and superscripts

c = cake or slurry side cake surface
d = deposition
e = erosion or outer (effluent) filter surface
i = species
l = carrier phase (liquid)
p = particle
p_1 = large particles
p_2 = small particles
w = inner filter surface
σ = dividing surface

Mathematical symbols

$-$ = mean value

Literature Cited

Abboud, N. M., "Formation of Filter Cakes with Particle Penetration at the Filter Septum," *Partic. Sci. and Technol.*, **11**, 115 (1993).
Adin, A., "Prediction of Granular Water Filter Performance for Optimum Design," *Filtr. and Separ.*, **15**, 55 (1978).
Arshad, S. A., "A Study of Surfactant Precipitation in Porous Media with Applications in Surfactant-Assisted Enhanced Oil Recovery Processes," PhD Diss., Univ. of Oklahoma, 285 pp. (1991).
Chase, G. G., and M. S. Willis, "Compressive Cake Filtration," *Chem. Eng. Sci.*, **47**, 1373 (1992).
Chen, W., "Solid-Liquid Separation via Filtration," *Chem. Eng.*, **104**, 66 (Feb., 1997).
Civan, F., "A Multi-Phase Mud Filtrate Invasion and Well Bore Filter Cake Formation Model," *Proc. SPE Int. Petroleum Conf. and Exhibition of Mexico*, Véracruz, Mexico, Paper SPE 28709, p. 399 (Oct. 10–13, 1994).
Civan, F., "A Multi-Purpose Formation Damage Model," *Proc. SPE Formation Damage Control Symp.*, Lafayette, LA, Paper SPE 31101, p. 311 (Feb. 14–15, 1996).
Civan, F., "Incompressive Cake Filtration: Mechanism, Parameters, and Modeling," *AIChE J.*, **44**(10), 2379 (1998).
Clark, P. E., and O. Barbat, "The Analysis of Fluid-Loss Data," *Proc. SPE Joint Rocky Mountain Regional/Low Permeability Reservoirs Symposium and Exhibition*, Denver, CO, Paper SPE 18971, p. 437 (Mar. 6–8, 1989).

Corapcioglu, M. Y., and N. M. Abboud, "Cake Filtration with Particle Penetration at the Cake Surface," *SPE Reservoir Eng.*, **5**, 317 (Aug. 1990).
Dake, L. P., *Fundamentals of Reservoir Engineering*, Elsevier, New York (1978).
Fehlberg, E., "Low-Order Classical Runge-Kutta Formulas with Stepsize Control and their Application to Some Heat Transfer Problems," NASA TR R-315, Huntsville, AL (July 1969).
Jones, S. C., and W. O. Roszelle, "Graphical Techniques for Determining Relative Permeability from Displacement Experiments," *J. Petrol. Technol. Trans. AIME*, **265**, 807 (1978).
Liu, X., and F. Civan, "Formation Damage and Filter Cake Buildup in Laboratory Core Tests: Modeling and Model-Assisted Analysis," *SPE Formation Evaluation J.*, **11**, 26 (1996).
Metzner, A. B., and J. C. Reed, "Flow of Non-Newtonian Fluids—Correlation of the Laminar, Transition, and Turbulent Flow Regions," *AIChE J.*, **1**, 434 (1955).
Potanin, A. A., and N. B. Uriev, "Micro-Rheological Models of Aggregated Suspensions in Shear Flow," *J. Coll. Int. Sci.*, **142**, 385 (1991).
Ravi, K. M., R. M. Beirute, and R. L. Covington, "Erodability of Partially Dehydrated Gelled Drilling Fluid and Filter Cake," *Proc. Technical Conf. and Exhibition of SPE*, Washington, DC, Paper SPE 24571, p. 219 (Oct. 4–7, 1992).
Sherman, N. E., and J. D. Sherwood, "Cross-Flow Filtration: Cakes with Variable Resistance and Capture Efficiency," *Chem. Eng. Sci.*, **48**, 2913 (1993).
Smiles, D. E., and J. M. Kirby, "Compressive Cake Filtration—A Comment," *Chem. Eng. Sci.*, **48**, 3431 (1993).
Tien, C., R. Bai, and B. V. Ramarao, "Analysis of Cake Growth in Cake Filtration: Effect of Fine Particle Retention," *AIChE J.*, **43**, 33 (1997).
Tiller, F. M., and J. R. Crump, "Recent Advances in Compressible Cake Filtration Theory," *Mathematical Models and Design Methods in Solid-Liquid Separation*, A. Rushton, ed., Martinus Nijhoff, Dordrecht (1985).
Xie, X., and D. D. Charles, "New Concepts in Dynamic Fluid-Loss Modeling of Fracturing Fluids," *J. Petrol. Sci. Eng.*, **17**, 29 (1997).

Appendix A: Thickness-Averaging Rules

The average of a quantity f over the radial distance extending between two radii r_c and r_w is defined by

$$\bar{f} = \int_{r_c}^{r_w} f d(\pi r^2) / (\pi r^2)|_{r_c}^{r_w} \tag{A1}$$

Thus, the following expressions used in the radial averaging can be derived similar to Civan (1994)

$$\int_{r_c}^{r_w} \frac{1}{r} \frac{\partial}{\partial r}(rf) d(\pi r^2) = 2\pi (rf)|_{r_c}^{r_w} \tag{A2}$$

$$\int_{r_c}^{r_w} \frac{\partial f}{\partial t} d(\pi r^2) = \frac{\partial}{\partial t}\left[\bar{f}(\pi r^2)|_{r_c}^{r_w}\right] - \left[f \frac{\partial}{\partial t}(\pi r^2) \right]\Bigg|_{r_c}^{r_w} \tag{A3}$$

Note that, in Eqs. A1 to A3, $r_c = r_c(t)$, Eq. A3 is an application of Leibnitz's rule, and Eqs. A1 to A3 can be applied to linear filtration by applying Eq. 31 for transformation from radial to linear flow cases.

Appendix B: Thickness-Averaged Fluid Pressure

The average fluid pressure in the filter cake for linear filtration can be expressed similar to Dake (1978) as

$$\bar{p} = \int_{x_c}^{x_w} p\phi dx \Bigg/ \int_{x_c}^{x_w} \phi dx \tag{B1}$$

The average cake porosity is given by

$$\bar{\phi} = \int_{x_c}^{x_w} \phi dx \Bigg/ \int_{x_c}^{x_w} dx \tag{B2}$$

The following expression can be derived from Eqs. B1 and B2

$$\bar{p}\bar{\phi} = \int_{x_c}^{x_w} p\phi dx \Bigg/ \int_{x_c}^{x_w} dx \tag{B3}$$

Note that x_w is a constant, but $x_c = x_c(t)$ varies by time.

Equation B3 defines the average fluid pressure, but it cannot be used directly, because the pressure distribution over the cake thickness is not known *a priori*. This problem can be circumvented by applying a procedure similar to Jones and Roszelle (1978) to express a local function value in terms of its average. Thus, Eqs. B2 and B3 can be differentiated to yield, respectively

$$\phi_c = \bar{\phi} + h\frac{d\bar{\phi}}{dh} \tag{B4}$$

$$p_c\phi_c = \bar{p}\bar{\phi} + h\frac{d(\bar{p}\bar{\phi})}{dh} \tag{B5}$$

in which h is the cake thickness given by Eq. 31. Eliminating the cake porosity ϕ_c at the slurry side cake surface between Eqs. B4 and B5 leads to the following expression that can be used to numerically calculate the average fluid pressure

$$\bar{p}\bar{\phi} + h\frac{d(\bar{p}\bar{\phi})}{dh} = p_c\left(\bar{\phi} + h\frac{d\bar{\phi}}{dh}\right) \tag{B6}$$

where p_c is the slurry pressure and $\bar{\phi}$ is given by Eq. 57.

Equations B1 through B6 can be transformed from linear to radial flow cases by applying Eq. 31.

Manuscript received Dec. 15, 1997, and revision received Sept. 3, 1998.